Structural Effects on Dynamic Features of Sandwich Metal/Polymer/Metal

P. CUILLERY,[1] R. GAERTNER,[1] J. TATIBOUET,[1] M. MANTEL[2]

[1]Groupe d'Etudes de Métallurgie Physique et de Physique des Matériaux, INSA de Lyon, 69621 Villeurbanne, France

[2] Centre de Recherche d'Ugine, Ugine S.A., 73403 Ugine, France

Received 19 July 1996; accepted 12 December 1996

ABSTRACT: A theoretical approach to the mechanical coupling between phases in metal/polymer/metal sandwich composites is developed assuming perfect interfaces. Comparisons between experimental dynamic mechanical spectroscopy and theoretical results are made with special attention to the geometrical characteristics. Unexpected results concerning the dependence on the width of the specimen are explained using the strain energy method. The polymer thickness influence is explained only by structural effects instead of the interface effects often found in the literature. The temperature of the sandwich loss factor peak is revealed to greatly depend on the specimen dimensions.
 J Appl Polym Sci **65:** 2493–2505, 1997

Key words: sandwich; viscoelasticity; torsion; interface; damping

INTRODUCTION

Vibrations damping and sonic insulation are the main applications of metal/polymer/metal sandwich composite materials. A search for high-damping materials entails the study of the damping properties of the composite as functions of the viscoelastic characteristics of the polymer.

Dynamic mechanical spectroscopy (DMS) is widely performed to characterize the viscoelastic comportment of composite materials. Experimental data exhibit that the maximum damping peak corresponding to the main mechanical relaxation of the polymer may be radically modified when polymer is included in the sandwich structure.[1–3] From a theoretical point, this modification can result from two phenomena:

1. the coupling that exists when the different phases (metal, polymer) are mechanically sollicited in the composite structure and
2. the modifications of the polymer morphology that may occur when building the composite structure.

Prior to any study or interpretation of the effects induced by modifications of the polymer morphology (interfaces, interphase creation), it is obvious that the effects related to the mechanical coupling of the different phases should be studied.

In this work we propose a theoretical approach to the mechanical coupling between phases in a sandwich composite structure when submitted to torsion deformation mode. The theoretical model is developed using the assumption of perfect interfaces. A comparison between theoretical results and experimental data issued from DMS experiments is presented, with special attention to the geometrical characteristics of the structure. To validate our analytical results, a comparison is also made with finite elements analysis. Finally,

Correspondence to: Dr. R. Gaertner.

Journal of Applied Polymer Science, Vol. 65, 2493–2505 (1997)
 CCC 0021-8995/97/122493-13

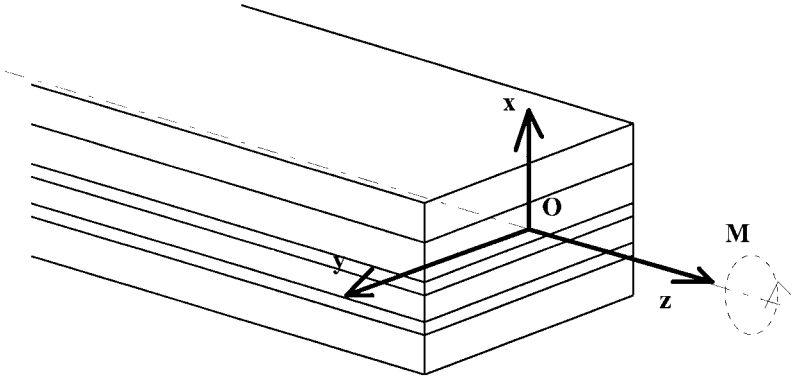

Figure 1 Torsion of multilayer beam with orthotropic layers; *Oz* is the torsion axis.

the problem is discussed in terms of stored and dissipated energy in the polymer layer.

THEORETICAL

The considered theoretical model is derived from classical arguments in the theory of viscoelasticity. After the stiffness determination of the composite beam, assuming that all the layers exhibit perfect elastic properties, the elastic moduli are replaced by the dynamical complex moduli according to the pinciple of correspondence[4] and the complex stiffness is then obtained. The ratio of the imaginary part to the real one is related to the damping coefficient of the material.

General Equations

We consider a laminated beam composed of orthotropic layers loaded in pure torsion mode as illustrated in Figure 1. The beam is referred to as a right-handed orthogonal coordinate system (O, x, y, z) where the Ox, Oy axis lies in the rectangular cross section with respect to its symmetries. For each layer the orthotropic axis is assumed to coincide with the reference axis. Moreover, the interfaces between the different materials are perfect (i.e., stresses and displacements are continuous through the interfaces).

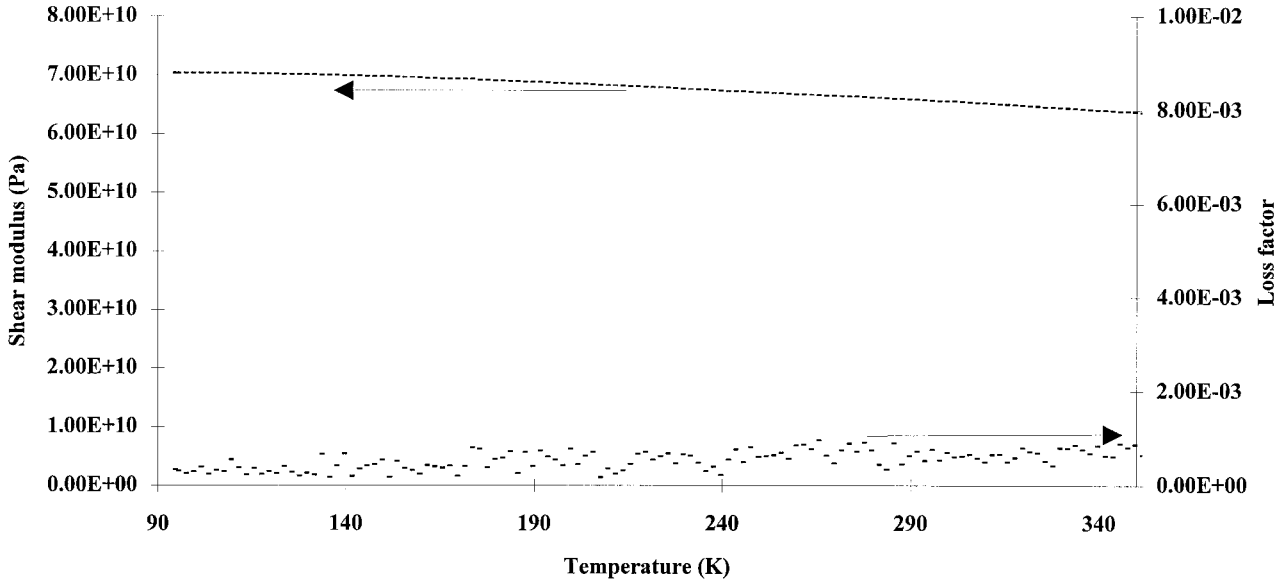

Figure 2 Temperature dependence of shear modulus and loss factor of the 304 stainless steel sheet.

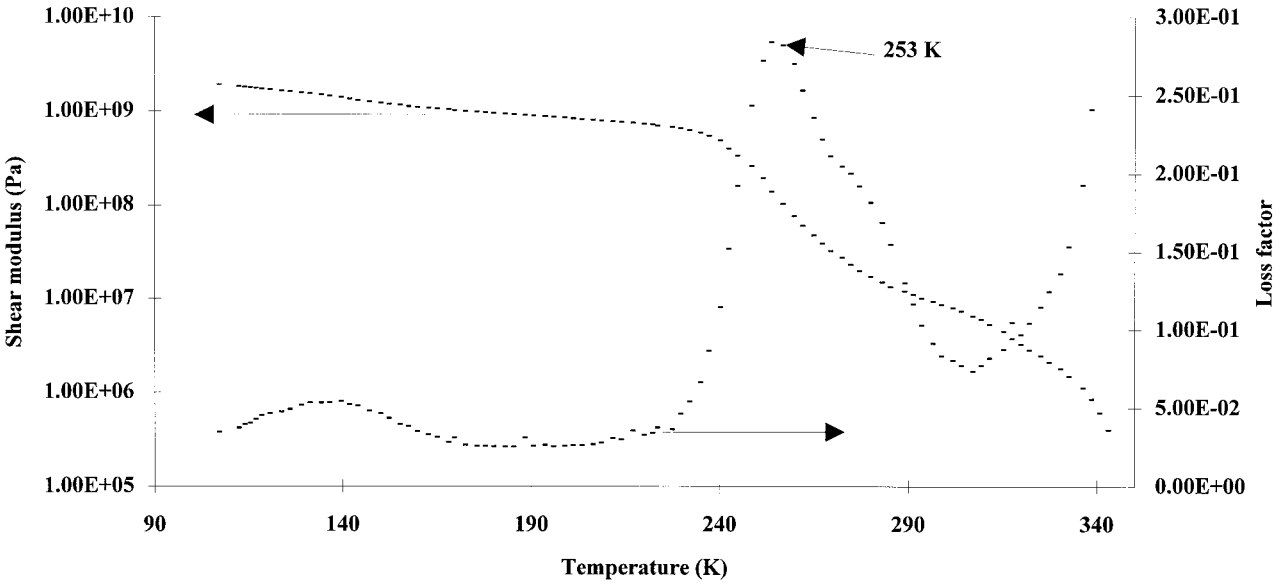

Figure 3 Temperature dependence of shear modulus and loss factor of the EVA polymer.

As is usual in the analysis of uniform torsion problems, we assume that all the transverse sections remain undeformed in their planes and that an axial warping occurs. Then, the displacement field can be expressed in the form

$$u = -\gamma \cdot z \cdot y, \quad v = \gamma \cdot z \cdot x, \quad w = \gamma \cdot \psi(x, y) \quad (1)$$

where γ is the relative torsion angle and $\psi(x, y)$ is the warping function.

The corresponding stress components of the ith layer are then

$$\sigma_{xz}^i = G_{xz}^i \cdot \varepsilon_{xz}^i$$
$$\sigma_{yz}^i = G_{yz}^i \cdot \varepsilon_{yz}^i \quad (2)$$

where G_{xz}^i and G_{yz}^i denote the shear moduli of the ith layer, respectively, relative to the xz and yz planes.

Far from the resonance frequency, the equilibrium equations reduce to

$$\frac{\partial \sigma_{xz}}{\partial x} + \frac{\partial \sigma_{yz}}{\partial y} = 0 \quad (3)$$

Substituting to $\psi(x, y)$ in the function $\varphi(x, y) = \psi(x, y) + x - y$ in the previous equation, we obtain

$$\frac{\partial^2 \varphi}{\partial x^2} + \frac{\partial^2 \varphi}{\partial y^2} = 0 \quad (4)$$

In each S_i area, the function φ is a solution of eq. (4) associated with the following boundary conditions: the external faces of the beam are free of stresses and the displacements and stresses are continuous through the interfaces between layers.

Then, the applied torque M can be obtained by integrating the moment of each force in regard to the torsion axis.

$$M = \int_S (-y \cdot \sigma_{xz} + x \cdot \sigma_{yz}) ds$$
$$M = \sum_i \int_{S_i} \gamma \cdot G_i \left(x^2 + y^2 + x \frac{\partial \varphi}{\partial y} - y \frac{\partial \varphi}{\partial x} \right) ds \quad (5)$$

Determination of Warping Function

The difficulty in this problem is to solve eq. (4). Some solutions are available in the literature for specific cases such as the two-layer beam,[5] the orthotropic beam,[6] and the symmetrical multilayer beam.[7,8] Recently generalization to the case of nonsymmetrical laminates was conducted simultaneously by different authors.[9,10] To solve this problem, we used[3] the warping function in the form proposed by Muskhelishvili[5]:

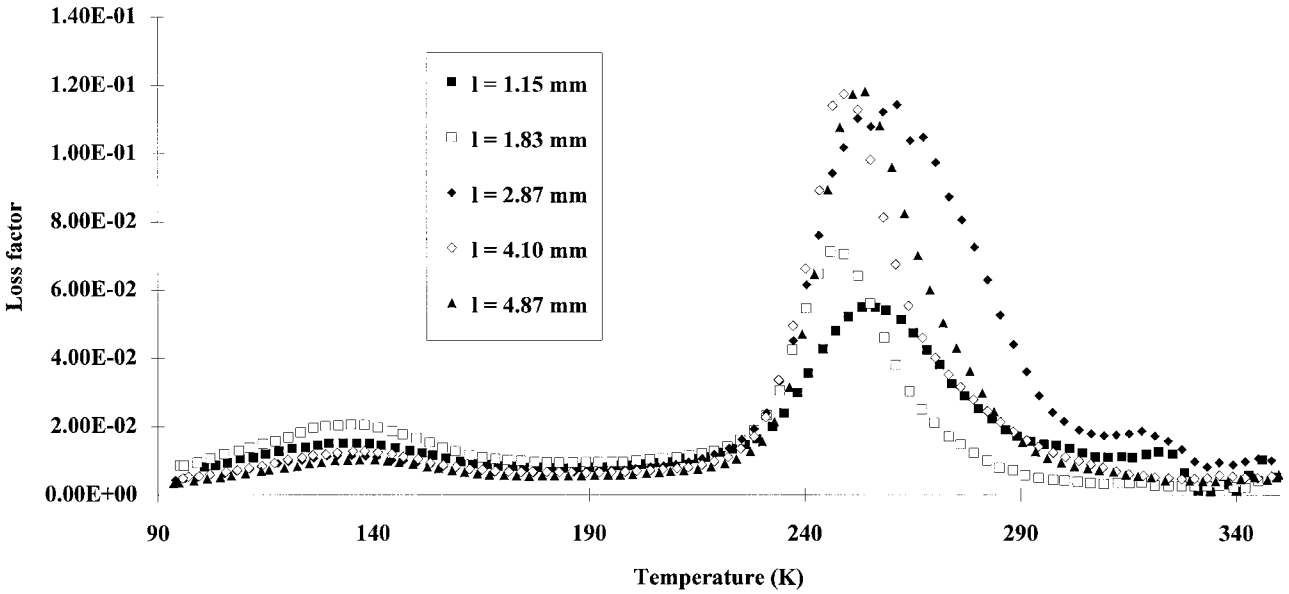

Figure 4 DMS experiments: temperature dependence of loss factor of sandwiches versus the specimen width l. The polymer thickness is 140 μm.

$$\varphi_i = \sum_{n=0}^{+\infty} (A^i_{2n+1} shmx + B^i_{2n+1} chmx) \sin my \quad (6)$$

$$m = \frac{(2n+1)\pi}{2c}$$

where c is the width and φ_i is the form taken by φ on S_i. The unknowns A^i_{2n+1} and B^i_{2n+1} could be calculated thanks to the boundaries conditions.

Finite Element Validation

This analytical approach is validated by the finite element method. Calculation of the warping field in the cross-section of the elastic sandwich beam loaded by a torsion torque is led by using a finite element program previously developed for ski studies and allowing for any kind of heterogeneity and load.[11] The real part of the analytical results is then

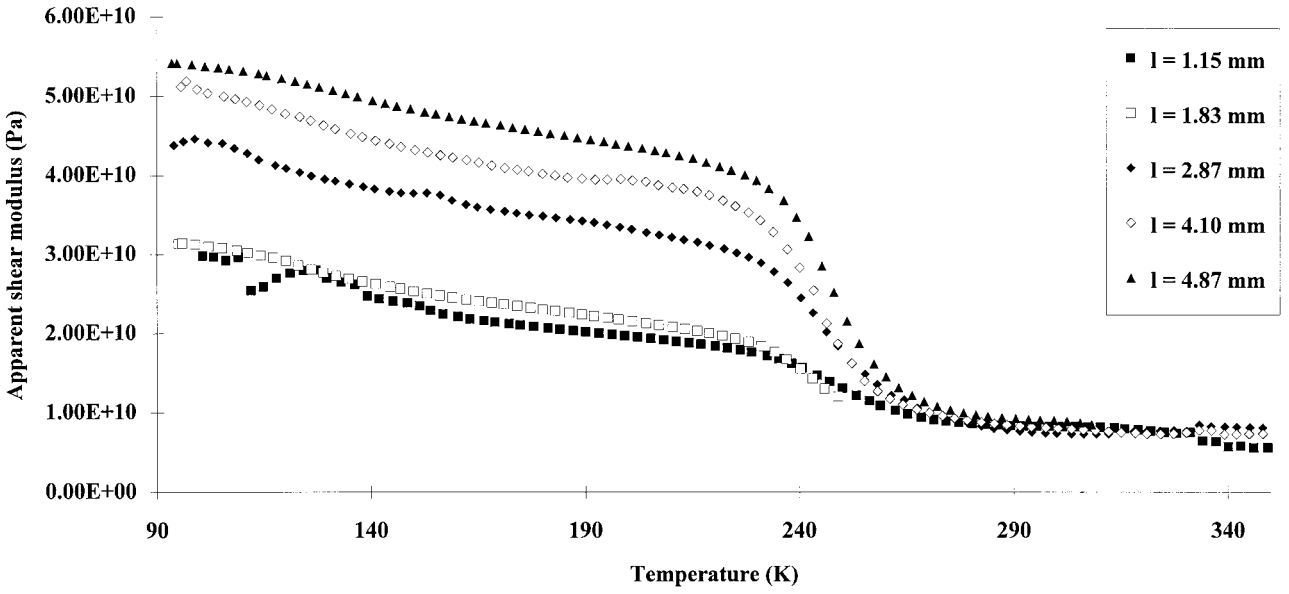

Figure 5 DMS experiments: temperature dependence of apparent shear modulus of sandwiches versus the specimen width l. The polymer thickness is 140 μm.

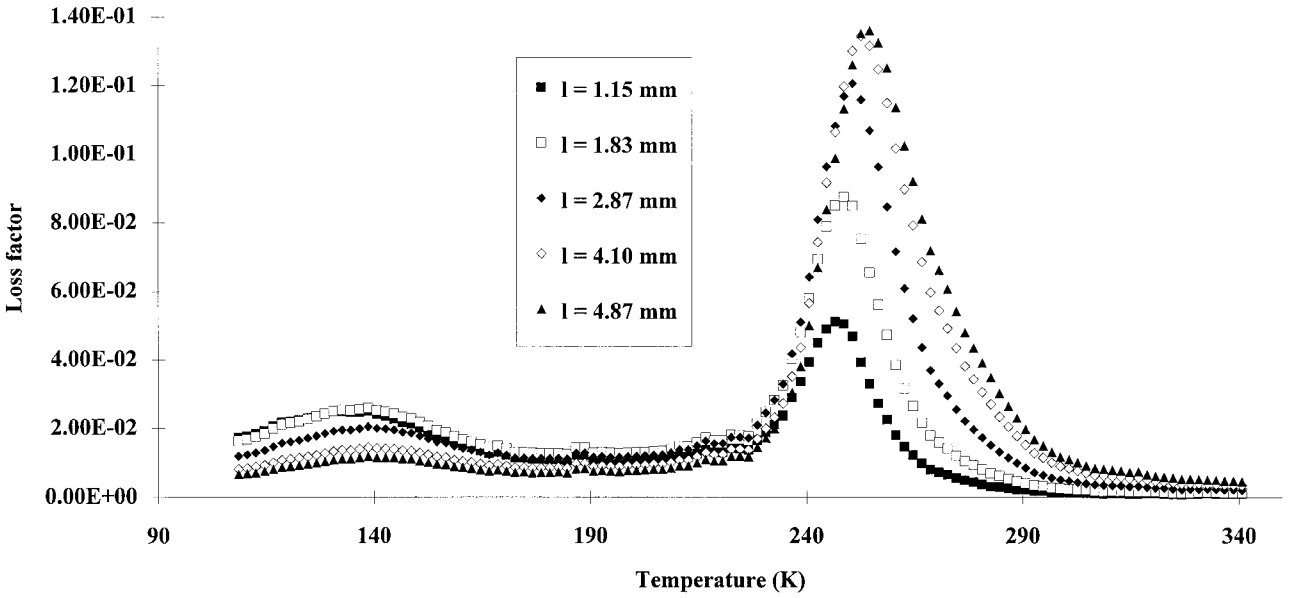

Figure 6 Analytical calculations: temperature dependence of loss factor of sandwiches versus the specimen width l. The polymer thickness is 140 μm.

systematically compared to the equivalent shear modulus resulting from this finite element analysis.

EXPERIMENTAL

DMS

Experiments are performed using an inverted torsion pendulum operating in forced oscillations.[12] For homogeneous and isotropic specimen, the torsion modulus is obtained as the ratio of the specimen stiffness to a geometric form factor depending on the specimen dimensions. In the case of the composite laminate beam, an apparent modulus is then obtained that corresponds to the torsion modulus of an isotropic homogeneous specimen with the same stiffness and geometry as the composite. The damping coefficient is defined as $\tan \delta = G''/G'$. Measure-

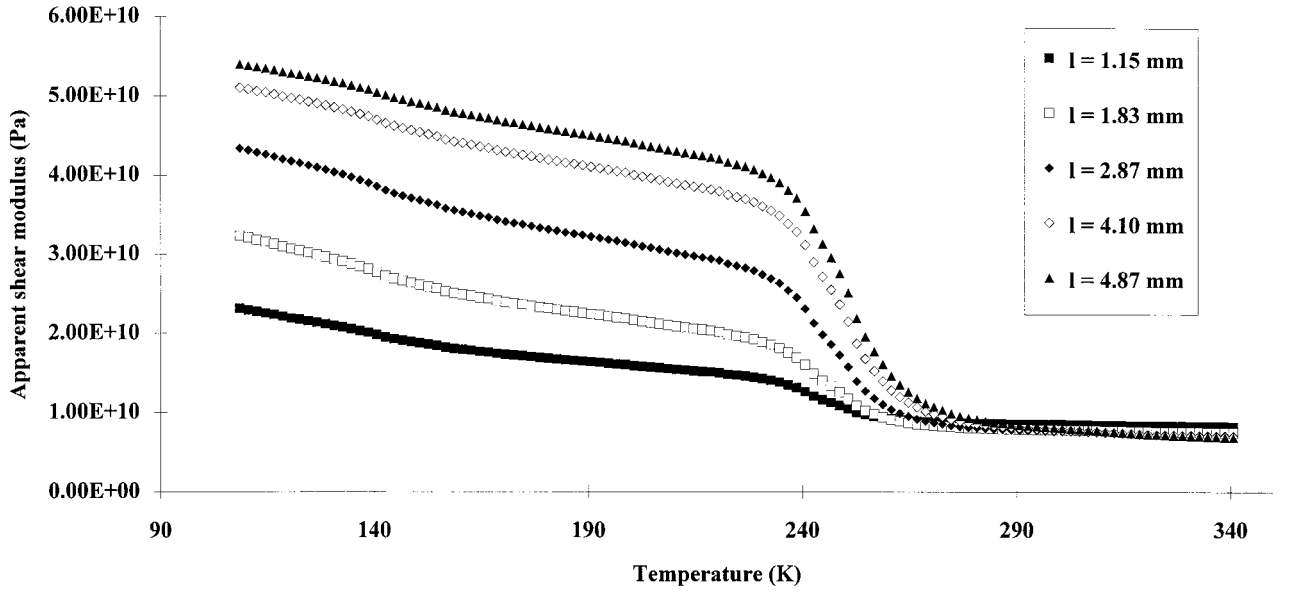

Figure 7 Analytical calculations: temperature dependence of apparent shear modulus of sandwiches versus the specimen width l. The polymer thickness is 140 μm.

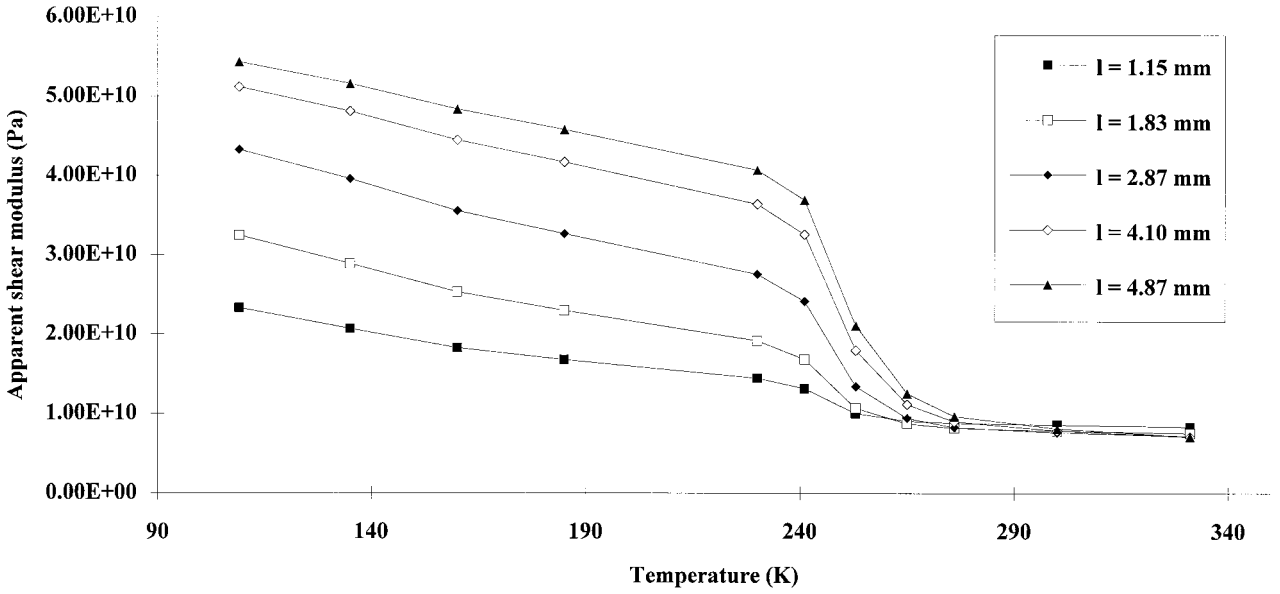

Figure 8 Finite elements calculations: temperature dependence of apparent shear modulus of sandwiches versus the specimen width l. The polymer thickness is 140 μm.

ments are done at 1 Hz with a heating rate of 1 K/min. The shear modulus of the polymer is normalized to 2 GPa at 100 K.

Materials

The metallic part of the sandwich is a sheet of stainless steel (Ugine S.A., 304 AISI) 200 μm thick. A normalized surface state is obtained by an annealing treatment at 850°C in a nonoxidant atmosphere (H_2/N_2). Figure 2 shows the dynamic mechanical characterization of the sheet. The damping coefficient remains constant and equals 6×10^{-4}. The torsion modulus exhibits a quasilinear evolution with temperature with a value of 66 GPa at 20°C.

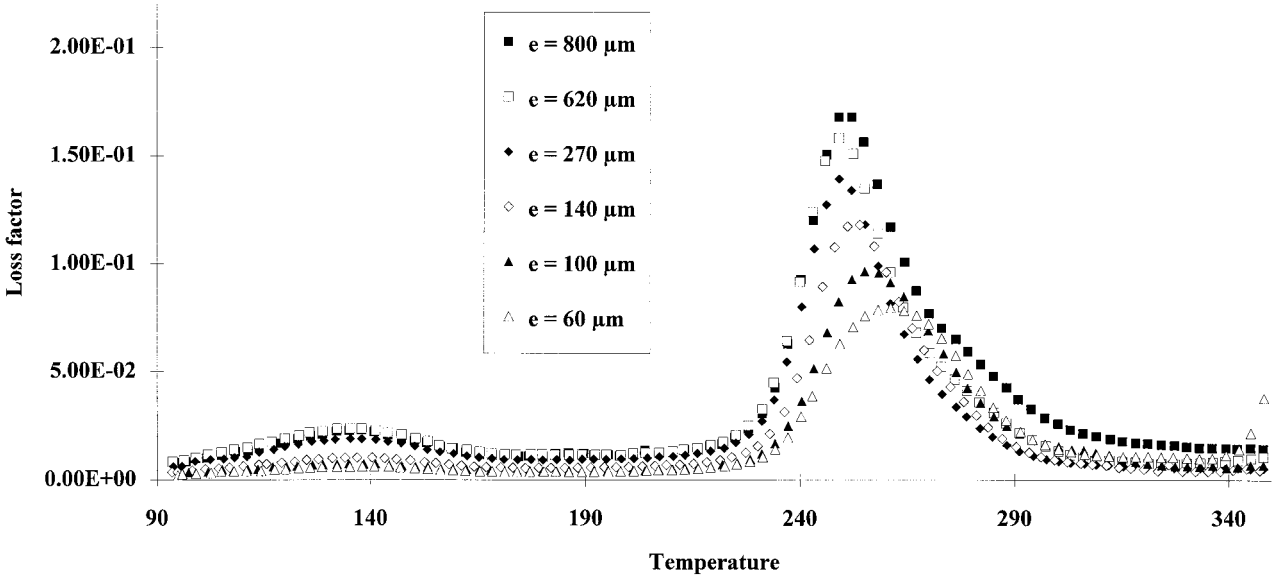

Figure 9 DMS experiments: temperature dependence of loss factor of sandwiches versus the polymer thickness e. The specimen width is 5 mm.

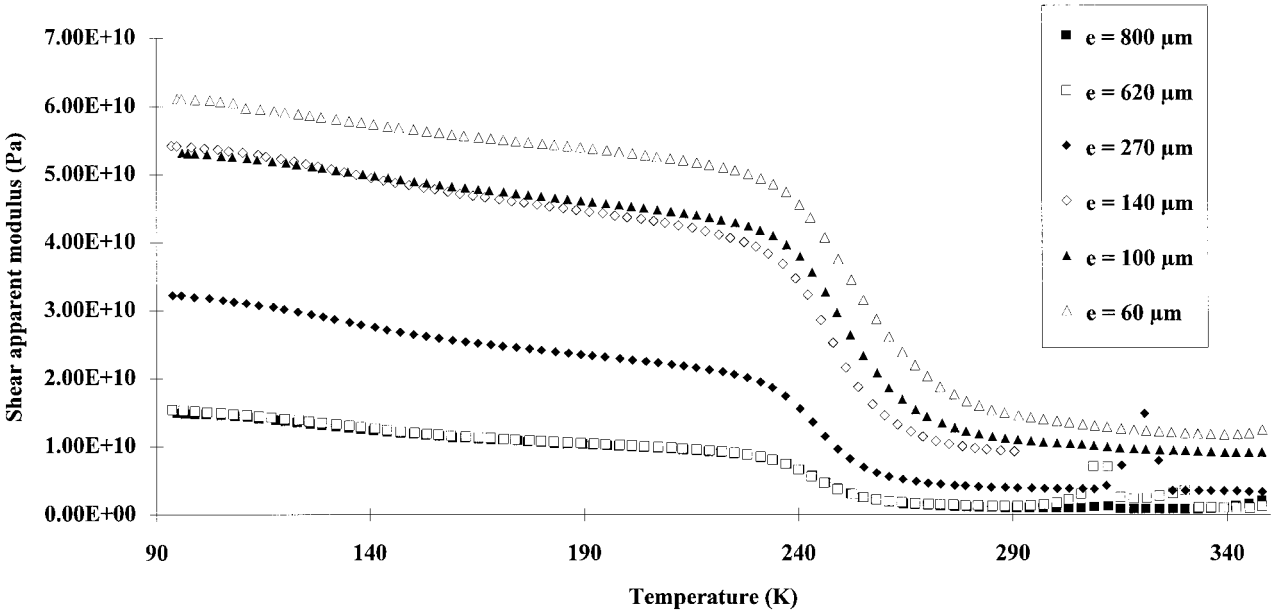

Figure 10 DMS experiments: temperature dependence of apparent shear modulus of sandwiches versus the polymer thickness e. The specimen width is 5 mm.

The considered polymer involved in the sandwich structure is a copoly(ethylene–vinyl acetate) (EVA, Orevac, Atochem). This semicrystalline polymer is maleic anhydride grafted to obtain good adhesion to the stainless steel. The viscoelastic features of EVA have been previously reported.[13] Dynamic mechanical characterization of this material is presented in Figure 3. This material exhibits a main mechanical relaxation at 253 K and a secondary one at 132 K for a 1-Hz frequency.

Processing of the sandwich is achieved by hot

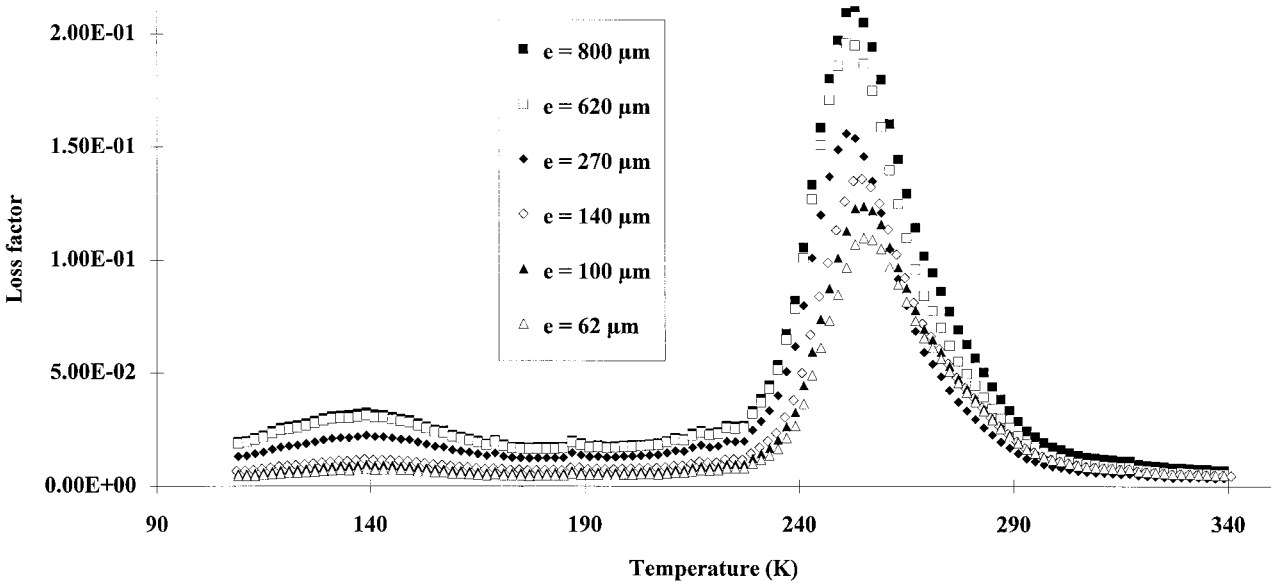

Figure 11 Analytical calculations: temperature dependence of loss factor of sandwiches versus the polymer thickness e. The specimen width is 5 mm.

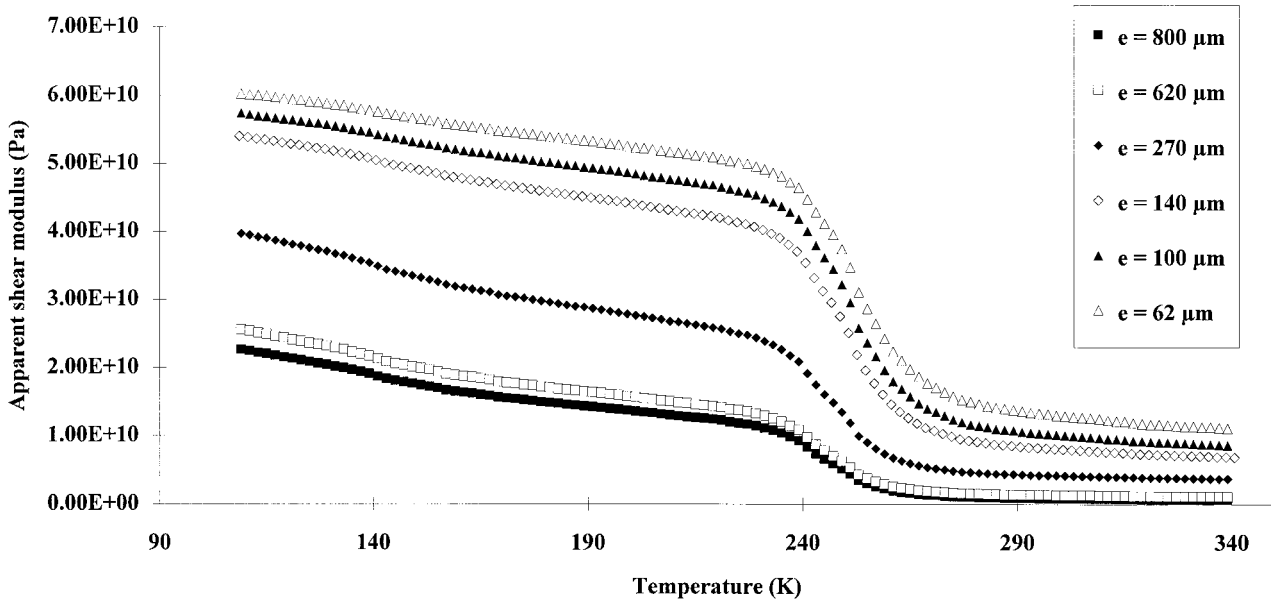

Figure 12 Analytical calculations: temperature dependence of apparent shear modulus of sandwiches versus the polymer thickness e. The specimen width is 5 mm.

pressing stainless steel sheets and polymer film under 0.1 MPa pressure at 200°C during 10 min. The sheet surfaces are cleaned prior the operation. The adhesion metal/polymer has been characterized[14] to confirm the assumption of perfect interfaces. Parallelepipedic specimens are carefully machined using a wire saw to maintain the geometry and in particular to avoid contacts between metal sheets at the edges of the specimens.

EXPERIMENTAL VERSUS THEORETICAL

Looking at the eq. (5) derived from the theoretical model, stiffness or apparent modulus of the sand-

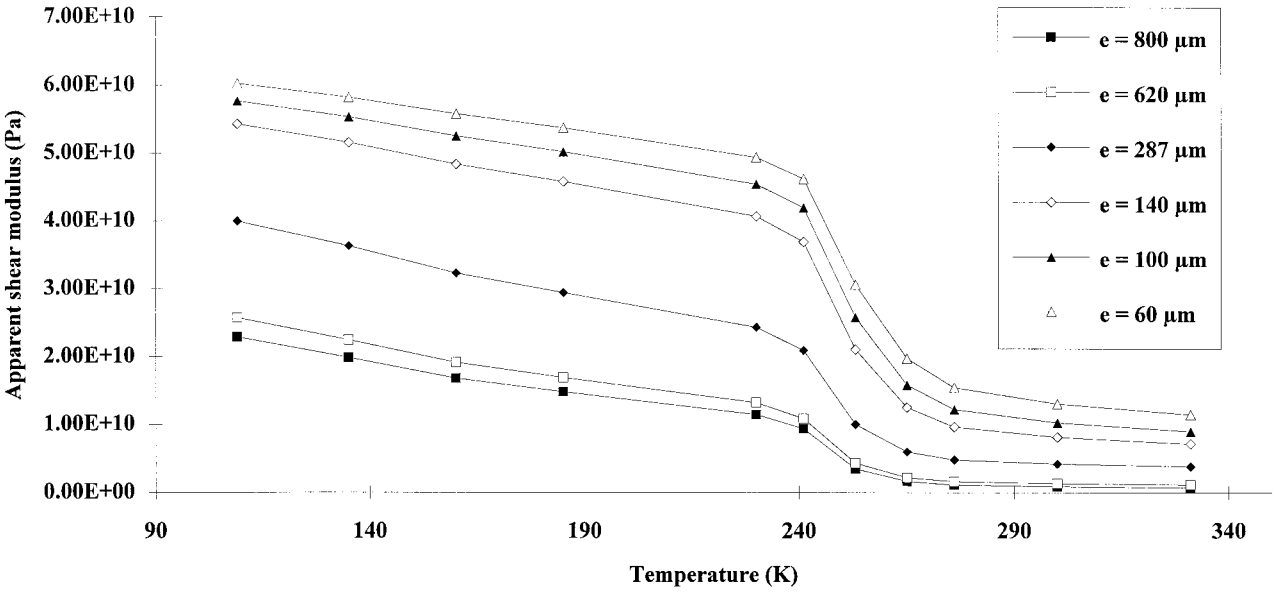

Figure 13 Finite elements calculations: temperature dependence of apparent shear modulus of sandwiches versus the polymer thickness e. The specimen width is 5 mm.

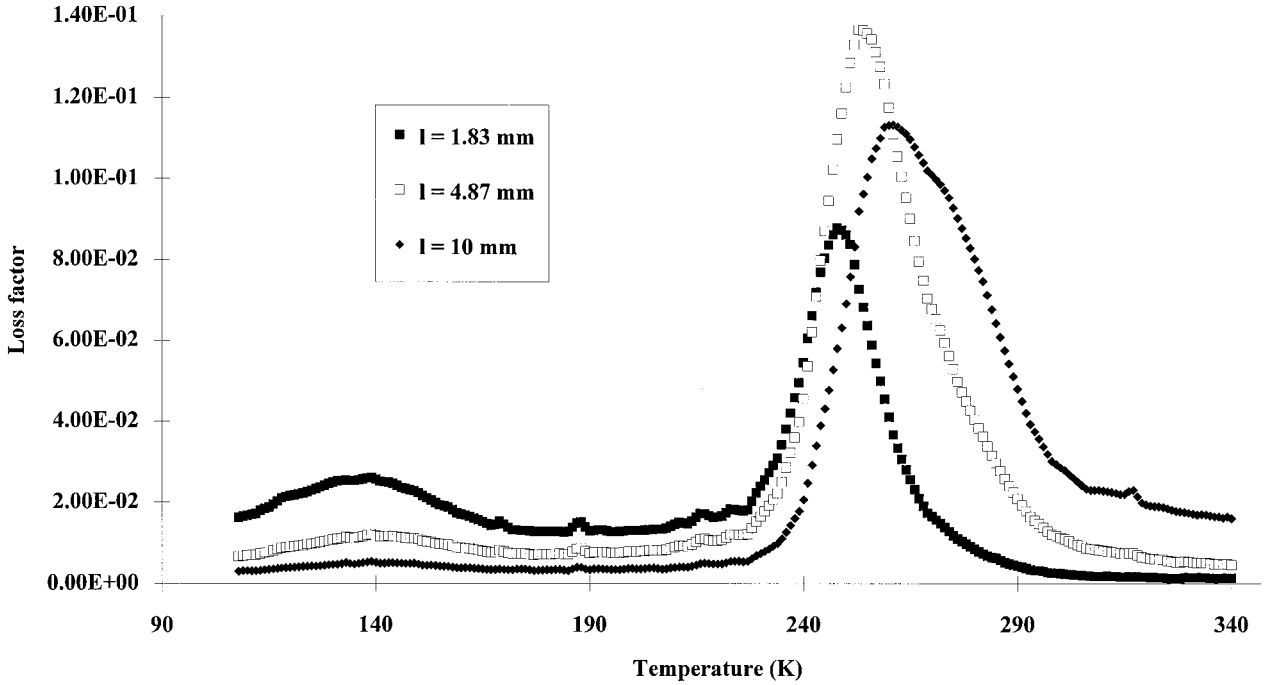

Figure 14 Analytical calculations: temperature dependence of loss factor of three sandwiches versus the specimen width l. The polymer thickness is 140 μm.

wich beam is dependent on the geometrical characteristics of the composite. In particular the width of the specimen and the polymer thickness relative to the stainless steel sheet thickness appear as important parameters. Comparisons between theoretical results and experimental ones are made by separately varying these parameters.

Dependence on Width of Specimen

Six specimens (constant polymer thickness 140 μm) with width varying from 1.15 to 4.87 mm were tested. The experimental damping coefficient and apparent modulus measured at 1 Hz are shown in Figures 4 and 5. Corresponding theoretical results are represented in Figures 6 and 7.

Concerning damping coefficient and loss modulus, four important features can be noticed:

1. The amplitude of the peak related to the secondary relaxation of the polymer decreases when width increases. The temperature of its maximum is shifted toward a low temperature.
2. The temperature of the maximum main loss peak increases with increasing width. This theoretical result is not so evident when looking at the experimental results.
3. The variation of the apparent modulus during the mechanical relaxation is proportional to the sample width.
4. At low temperature the apparent modulus increases when the width increases. But at high temperature the apparent modulus decreases when the width increases. The theoretical results are accurate enough to interpret a result that apparently looks like an experimental artifact.

The finite elements calculations concerning the apparent shear modulus are shown Figure 8. These calculations validate the analytical results presented Figure 7 with a good accuracy.

Dependence on Polymer Thickness

To study the polymer thickness influence, six specimens are processed with a central layer thickness varying from 60 to 800 μm. The polymer thickness influence on the loss factor and apparent modulus are shown in Figures 9 and 10. These results should be compared to those obtained with the analytical model that are presented in Figures 11 and 12. A good correlation is obtained between the analytical results and the experimental ones. It leads to the following comments:

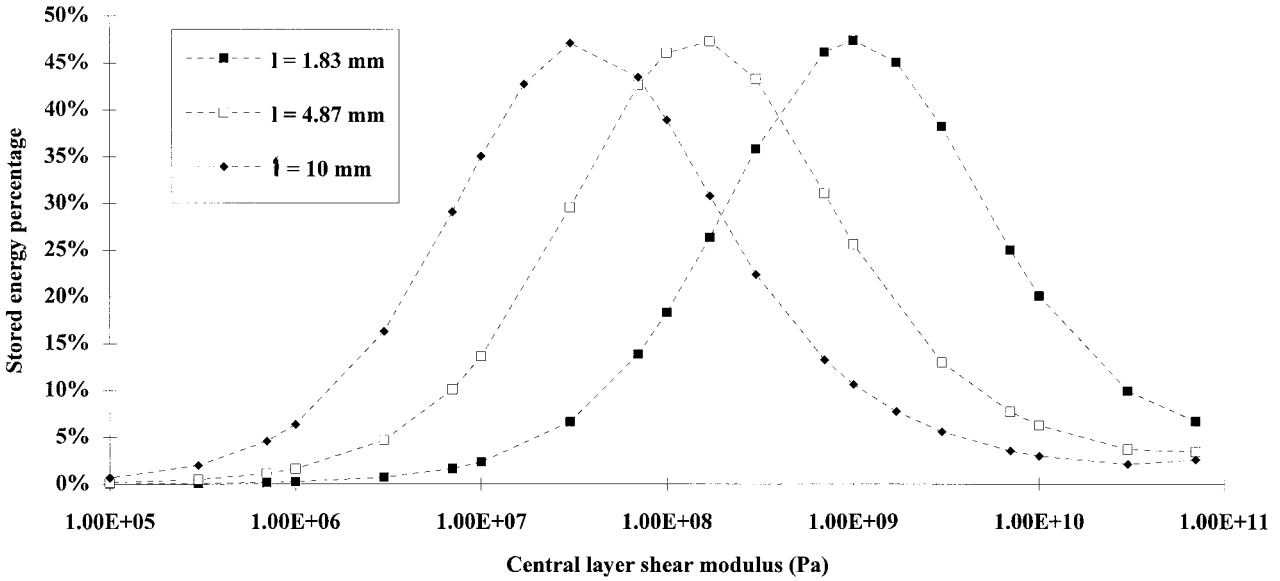

Figure 15 Central layer shear modulus dependence of the stored energy percentage versus the specimen width.

- The loss factor peaks related to both polymer mechanical relaxations grow when increasing the thickness.
- The thinner the polymer, the more the temperature of the loss peak maxima is shifted toward high temperature. This effect is not easy to reveal experimentally.
- Over the entire temperature range, the apparent modulus increases when decreasing the polymer thickness. Beyond 200 μm, this evolution slows down.

The analytical results concerning the apparent modulus (Fig. 12) are completely validated by the finite elements calculations as shown in Figure 13.

Discussion

An argument often found in the literature is that the thinner the polymer, the more important the volume fraction of the interphase is. That leads to attributing the polymer thickness influence on the multilayer loss peak to an interphase effect.[1,15,16] Furthermore, the temperature shift of the loss peak maximum is explained by strong interactions in the vicinity of the interface.[17,18] Our analysis shows that the polymer thickness influence and the temperature shift of the loss peak could be attributed only to a structural effect.

Generally, the experimental loss peak amplitude is slightly smaller than the theoretical one. In fact the boundaries conditions assumed by the model are not exactly the same as imposed during the experimental DMS test. The first condition assumes the right cross section warping to be unchanged over the entire length and the second one does not allow this warping at the end of the specimen. Therefore, an additional study seems necessary before considering any interfacial effects.

INTERPRETATION

The unexpected effect of the mechanical coupling is the width sample influence. The polymer thickness influence is easier to understand. Increasing the polymer volume fraction makes the sandwich behavior toward the polymer behavior. The loss factor increases and the apparent modulus decreases the stiffness of both metal foils.

On the other hand, the width sample influence is very surprising because without varying the polymer/metal volume ratio, great changes affect the mechanical relaxation peaks of the sandwiches. Furthermore, decreasing the width leads to an increase of the loss factor peak corresponding to the secondary polymer relaxation (about 140 K), although the inverse effect is revealed on the main loss factor peak

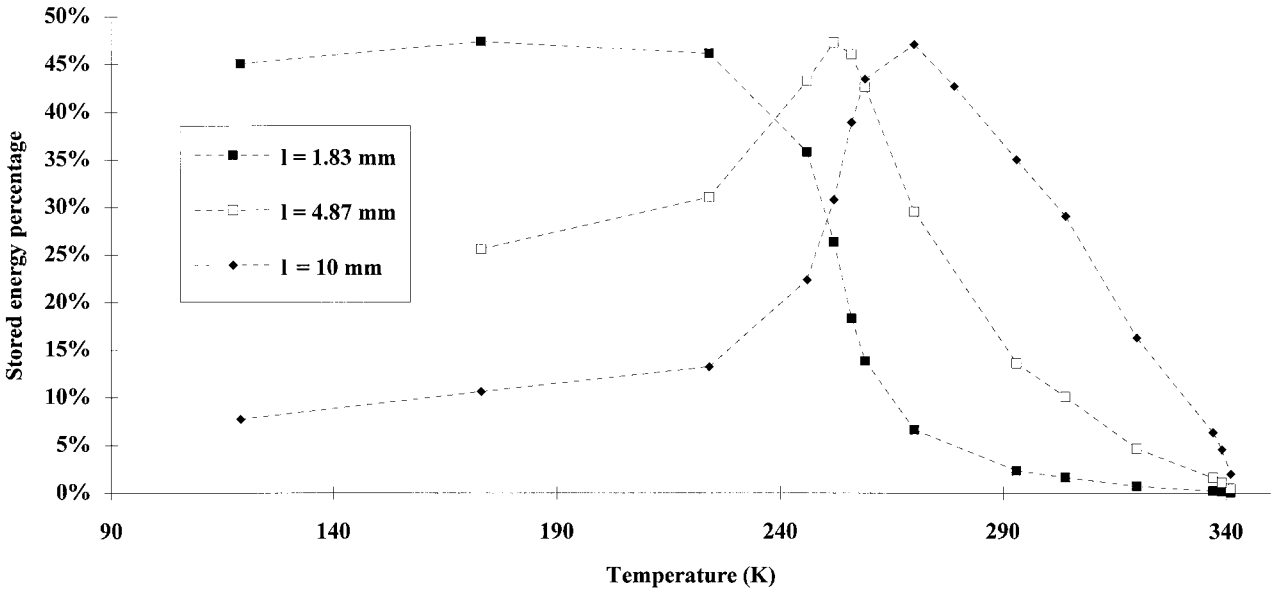

Figure 16 Temperature dependence of stored energy percentage versus the specimen width.

(about 250 K). A width decrease leads to a peak amplitude decrease.

Strain Energy Method

To understand these results, the sandwich loss factor should be calculated in terms of the energy fraction stored in each phase. The calculation could be conducted using the strain energy method.[19,20] The coordinates system is defined as follows: Oz is the torsion axis and Ox and Oy are chosen considering the sandwich right section symmetries. W^k is the energy received by the kth phase per unit length. This energy could be written as

$$W^k = \tfrac{1}{2}\int_{S_k} \sigma_{ij}^k \cdot \varepsilon_{ij}^k \cdot dS_k$$

$$W^k = \int_{S_k} [\sigma_{xz}^k \cdot \varepsilon_{xz}^k + \sigma_{yz}^k \cdot \varepsilon_{yz}^k] \cdot dS_k$$

$$W^k = 2\int_{S_k} G_k^* [(\varepsilon_{xz}^k)^2 + (\varepsilon_{yz}^k)^2] \cdot dS_k \qquad (7)$$

where ε_{ij}^k and σ_{ij}^k are, respectively, the strain and stress tensor components previously defined,[3] G_k^* is the complex shear modulus of the kth layer, and W^k could be split in a real part corresponding to the stored energy W_e^k and an imaginary part that is the dissipated energy W_d^k. So

$$W_e^k = 2 \cdot G_k' \int_{S_k} [(\varepsilon_{xz}^k)^2 + (\varepsilon_{yz}^k)^2] \cdot dS_k \qquad (8)$$

$$W_d^k = \eta^k W_e^k \qquad (9)$$

where η^k is the loss factor of the kth layer.

Notes that this approach assumes that each strain tensor component dissipates the energy independently from each other. The stored energy percentage of the kth layer is defined as

$$\%W_e^k = \frac{W_e^k}{\sum_i W_e^i} \qquad (10)$$

Then the sandwich loss factor $tg\,\delta$ could be determined using the stored energy percentage. The subscript s refers to the steel and p to the polymer.

$$tg\,\delta = \frac{W_d^s + W_d^p}{W_e^s + W_e^p} \qquad (11)$$

but

$$\%W_e^p = 1 - \%W_e^s, \quad W_e^k = \%W_e^k \cdot \sum_k W_e^k$$

and $W_d^k = \eta^k W_e^k$

That leads to

$$tg\delta = \%W_e^p \cdot (\eta^p - \eta^s) + \eta^s \qquad (12)$$

In our experiments, we have the conditions

$$\eta^s \ll \eta^p \quad \text{and} \quad \eta^s \ll tg\delta$$

The sandwich loss factor could be written as follows:

$$tg\delta \approx \%W_e^p \cdot \eta^p \qquad (13)$$

The sandwich loss factor is equal to the product of the percentage of the stored energy in the polymer by its loss factor. The difference between the loss factor determined by this method and the result obtained by the analytical model never exceeds 2% of the value.

Study of Width Sample Influence on Sandwich Loss Factor

Thanks to the model presented above, the dissipated and stored energy of each layer can be calculated. A Fortran program can determine the strain tensor components and the stored and dissipated energy in each point of the cross section of the composite. The calculation is performed using 294 points. Integrations on the right section area of each phase give the stored energy percentage of the central layer. The torsion angle per unit length γ is chosen to be 1 rd/m.

Three different sample widths are studied: 1.83, 4.87, and 10 mm. The first samples are studied theoretically (Figs. 4, 5). These results and those obtained for the 10-mm width sample are shown in Figure 14. The polymer thickness is 140 μm. The width increase always leads to a shift of the main relaxation peak toward high temperature. The amplitude of this peak goes through a maximum at 4.87-mm width and then decreases. The existence of this maximum has not been detected because the experimental device limits the sample geometry.

The stored energy percentage $\%W_e^p$ is calculated for the three samples. The stainless steel modulus is 70 GPa. Figure 15 shows the variation of this energy percentage versus the central layer modulus. It is easily seen that for each width $\%W_e^p$ goes through a maximum and this maximum is shifted toward low modulus with increasing width. For each width and more generally for each geometry an optimal value of the shear modulus corresponds to the greatest energy stored in the central layer. The maximum stored energy percentage is unchanged on the width range explored. Its value is 47%, although the central layer volume fraction is only 26%.

During a DMS test, the shear modulus of the polymer varies from 2 GPa at low temperature to 10^5 Pa at high temperature (Fig. 3). Each value of the polymer shear modulus corresponds to a particular value of $\%W_e^p$. Figure 16 shows the variation of $\%W_e^p$ with the temperature for the three structure geometries.

The sandwich loss factor has been calculated under a product form [see eq. (12)]. The loss factor is the product of the function $\%W_e^p(T)$ versus temperature (Fig. 16) and the function that describes the polymer loss factor variation with the temperature $\eta^p(T)$ (Fig. 3).

Now it is possible to explain the width sample influence on the TMS results. Figure 16 shows that at low temperature $\%W_e^p$ increases with decreasing width. At a constant temperature (at constant η^p), the composite loss factor increases when the width decreases.

The amplitude of the loss factor peak should not be greater in the case where the $\%W_e^p(T)$ and the $\eta^p(T)$ function maxima have the same temperature. In this case, the loss factor reaches its maximum value, which is 47% of the polymer loss factor maximum. Furthermore, any shift in temperature is revealed because both maxima take place at the same temperature. The 4.87-mm width sample represents this particular case.

The shift in temperature of the $\%W_e^p(T)$ function with increasing width explains the temperature shifts revealed between loss factor peaks.

The $\%W_e^p(T)$ maximum shift controls the peak amplitude. The latter increases to the point of coincidence discussed above and then decreases.

CONCLUSION

A good correlation is generally obtained between the analytical model results and the experimental tests. The stiffnesses determined by the model are confirmed by finite elements calculations. The modifications revealed between polymer mechanical relaxations and composite mechanical ones are mainly attributed to a structural effect. The model robustness outlines experimental problems (jaws influence, polymer creep, etc.) rather than interfaces effects often proposed in the literature.

In particular, the surprising results of the sample width influence were studied and interpreted with the strain energy method.

We thank Mr. F. Pourroy, 3S laboratory, INPG Grenoble, France, for helpful recommendations and advice in finite elements calculations.

REFERENCES

1. H. Bourahla, J. Chauchard, J. Lenoir, and M. Roman, *Angew. Makromol. Chem.,* **178,** 47 (1990).
2. J. Landier, P. Mercier, and M. Berveiller, *Rev. Compos. Matér. Av.,* **4,** 51 (1994).
3. P. Cuillery, L. David, S. Etienne, and M. Mantel, *J. Mater. Sci.,* **31,** 1915 (1996).
4. Z. Hashin, *Int. J. Solids Struct.,* **6,** 539 (1970).
5. N. I. Muskhelishvili, *Some Basic Problems of the Mathematical Theory of Elasticity,* P. Noordhoff Ltd., Groningen, The Netherlands, 1954.
6. S. G. Leknistskii, *Theory of Elasticity of an Anisotropic Elastic Body,* Mir, Moscow, 1981.
7. S. Cheng, X. Wei, and T. Jiang, *J. Eng. Mech.,* **115,** 1150 (1989).
8. J. M. Whitney and R. D. Kurtz, in *Proceedings of the American Society for Composites,* Tecnomic, Lancaster, PA, 1988.
9. J. M. Whitney and R. D. Kurtz, *Compos. Eng.,* **3,** 83 (1993).
10. M. Savoia and N. Tullini, *Compos. Struct.,* **25,** 587 (1993).
11. C. Clerc, R. Gaertner, and P. Trompette, *Finite Elements Anal. Des.,* **5,** 1 (1989).
12. S. Etienne, J. Y. Cavaillé, J. Perez, R. Point, and M. Salvia, *Rev. Sci. Instrum.,* **53,** 1251 (1982).
13. P. J. Cunat, M. Mantel, and P. Cuillery, *Méc. Matér. Electric.,* **21,** 21 (1992).
14. D. Maccarinelli, M. Mantel, B. Baroux, N. S. Prakash, M. Charbonnier, and M. Roman, in *EURAHD 92,* Dechema, Ed., Karlsruhe, Germany, 1992.
15. S. Bistac, M. F. Vallat, and J. Shultz, in *EURAHD 94,* Société Française du Vide, Ed., Mulhouse, France, 1994.
16. J. F. Gérard and P. Huchedé, in *Proceedings of the Sixteenth Annual Meeting and the International Symposium on the Interphase,* F. J. Boerio, Ed., Williamsburg, Virginia, 1993.
17. T. Bhattacharya, D. K. Tripathy, and S. K. De, *J. Adhes. Sci. Technol.,* **6,** 1165 (1992).
18. H. Mizumaki, *J. Adhesion,* **42,** 292 (1970).
19. S. J. Hwang and R. F. Gibson, *J. Eng. Mater. Technol.,* **109** 47 (1987).
20. C. D. Johnson and D. A. Kienholz, *AIAA J.,* **20,** 1284 (1982).